J Geod (2006) 80: 507–523
DOI 10.1007/s00190-006-0068-2

ORIGINAL ARTICLE

J.-M. Lemoine · H. Capdeville

A corrective model for Jason-1 DORIS Doppler data in relation to the South Atlantic Anomaly

Received: 14 January 2006 / Accepted: 26 May 2006 / Published online: 8 August 2006

Abstract The DORIS Doppler measurements collected by Jason-1 are abnormally perturbed by the influence of the South Atlantic Anomaly (SAA). The DORIS ultra-stable oscillators on-board Jason-1 are not as stable as they should be; their frequency is sensitive both to the irradiation rate and to the total irradiation encountered in orbit. The consequence is that not only are the DORIS measurement residuals higher than they ought to be, but also large systematic positioning errors are introduced for stations located in the vicinity of the SAA. In this paper, we present a method that has been devised to obtain a continuous observation of Jason-1 frequency offsets. This method relies on the precise determination of the station frequency and troposphere parameters via the use of other DORIS satellites. More than 3 years of these observations have then been used to construct a model of response of the oscillators of Jason-1 to the SAA. The sensitivity of the Jason-1 oscillators to the SAA perturbations has evolved over time, multiplied by a factor of four between launch and mid-2004. The corrective performances of the model are discussed in terms of DORIS measurement residuals, precise orbit determination and station positioning. The average DORIS measurement residuals are decreased by more than 7 % using this model. In terms of precise orbit determination, the 3D DORIS-only orbit error decreases from 5 to 4.2 cm, but the DORIS+SLR orbit error is almost unaffected, due to the already good quality of this type of orbit. In terms of station positioning, the model brings down the average 3D mono-satellite monthly network solution discrepancy with the International Terrestrial Reference Frame ITRF2000 from 11.3 to 6.1 cm, and also decreases the scatter about that average from 11.3 to 3.7 cm. The conclusion is that, with this model, it is possible to re-incorporate Jason-1 in the multi-satellite geodetic solutions for the DORIS station network.

Keywords DORIS · Doppler · South Atlantic Anomaly · Ultra-stable oscillator · Precise orbit determination · TOPEX/Poseidon · Jason-1 tandem phase

J.-M. Lemoine (✉)
CNES (Centre National d'Etudes Spatiales),
18, avenue Edouard Belin, 31401 Toulouse cedex 4, France
E-mail: Jean-Michel.Lemoine@cnes.fr
Tel.: +33-561553448
Fax: +33-561253098

H. Capdeville
CLS (Collecte Localisation Satellites),
8–10, rue Hermès, Parc Technologique du Canal,
31520 Ramonville-Saint-Agne, France
E-mail: hcapdeville@pop.cls.cnes.fr

1 Introduction

The NASA/CNES (US National Aeronautical and Space Administration/French Centre National d'Etudes Spatiales) Jason-1 satellite altimeter (Ménard et al. 2003), the successor of TOPEX/Poseidon (Fu et al. 1994), relies on a microwave altimeter providing a measurement of the distance between the satellite and the surface of the ocean, and on the precise and continuous positioning of the satellite above the Earth, particularly in the radial direction, providing the height of the satellite above the reference ellipsoid. For this purpose, Jason-1 uses three different and complementary tracking systems: Satellite Laser Ranging (SLR) retro-reflectors, Global Positioning System (GPS) receivers and DORIS (Doppler Orbitography and Radiopositioning Integrated by Satellite) receivers.

An anomalous behaviour of the DORIS ultra-stable oscillator (USO) on-board Jason-1 was first pointed out by Willis et al. (2003, 2004), who showed that the positioning of the DORIS stations located in the area of the South Atlantic Anomaly (SAA) was drifting away from the true position, either given by the ITRF2000 (International Terrestrial Reference Frame 2000, cf. Altamimi et al. 2002) or determined using data from other satellites carrying a DORIS receiver. The error for these contaminated stations can exceed 40 times the standard positioning error of the other stations.

The SAA is the area of the ionosphere where the Van Allen radiation belts are the closest to the surface of the Earth. These roughly toroidal belts, which trap charged particles, follow the magnetic equator. The Earth's magnetic centre is offset from the Earth's centre of mass by approximately 500 km towards Indonesia. Thus the ellipses described by the satellite orbits about the centre of mass of the Earth intersect the torus of the Van Allen belts along an oval-shaped area over Brazil. Closely connected to the Earth's magnetic field, the SAA changes with it and its location and shape slowly evolves over time. There is a slow westward drift of the SAA at the rate of 0.3 deg/year (Heynderickx 1996) and radially the geomagnetic dipole field drifts away from the centre of the Earth at a rate of about 2.5 km/year (Fraser-Smith 1987).

Oscillators on-board low Earth orbiting satellites can be affected by the high-energy protons present in the Van Allen belts (Armstrong and Colborn 1992; Badhwar et al. 1999). They can experience, in particular, a shift in their frequency. In the case of Jason-1, for which DORIS is the nominal tracking technique together with SLR, the stability of its oscillator, or at least the knowledge of its instantaneous frequency is crucial, not only in terms of station positioning (locally), but also in terms of orbit accuracy (globally).

There are two DORIS instruments onboard Jason-1 for redundancy reasons. From launch (December 7, 2001) until June 25, 2004, the redundant instrument (instrument n°2) was active. When the SAA-induced instability of the DORIS USO was first detected, that instrument was ON. As long as that instrument was active, the problems of station positioning using Jason-1 DORIS data kept on increasing with time. It triggered the present study, in order to assess if it was possible to identify, and hopefully correct, the effect of the SAA on the USO. The questions that had to be addressed were: Is it possible to find a way to observe, in a continuous manner, the frequency offset of Jason-1? If so, can a model, explicative and predictive, of the response of Jason-1 USO to the SAA be built?

On June 25, 2004, a switch from the redundant to the nominal instrument was carried out, and instrument n°1 has since been active. Instrument n°1 is also sensitive to the SAA, although to a lesser extent than instrument n°2 towards the end, and the scope of the present study has been extended to this new instrument.

In the first part of this paper, a diagnosis of the perturbation of the DORIS Jason-1 USO related to the SAA is performed; then a method for continuously observing the Jason-1 frequency offset is presented. The success of this method has allowed the construction of a model for the correction of the DORIS USOs and a determination of the model parameters over the whole life-span of Jason-1. One noticeable by-product of this study is a new map of the SAA, at the altitude of Jason-1. Finally, the impact of the model corrections on the quality of the DORIS data is discussed in terms of station positioning, data outlier reduction and orbit accuracy.

2 Doris data and precision orbit determination

DORIS is a well known Doppler tracking system designed by CNES with the participation of the Institut Géographique National (IGN) and the Groupe de Recherche de Géodésie Spatiale (GRGS) (Debaisieux et al. 1986; Tavernier et al. 2003). Following the example set up earlier by the IGS (International GNSS Service) and ILRS (International Laser Ranging Service), an International DORIS Service (IDS) was set up in 2003 by the International Association of Geodesy (IAG) (Tavernier et al. 2005). It supports the numerous scientific applications of DORIS in the fields of geodesy and geodynamics, among which are:

- Participation in the International Terrestrial Reference Frame (ITRF), the practical realization of the International Terrestrial Reference System (ITRS),
- Monitoring deformations of the solid Earth
- Monitoring vertical crustal deformation at tide gauges
- Monitoring variations in the hydrosphere (sea level, ice-sheets, etc.)
- Orbit determination for scientific satellites
- Ionospheric monitoring

DORIS is an uplink system, the transmitters being on the ground and the receivers on-board the satellites. A number of scientific satellites are equipped with DORIS receivers: the SPOT series (*Satellites Pour l'Observation de la Terre*) from SPOT-2 to SPOT-5, ENVISAT, TOPEX/Poseidon (T/P) and Jason-1. The DORIS system is monitored by two master beacons in Toulouse, France, and Kourou, French Guyana (three since mid-September 2005, with the addition of Hartebeesthoek, South Africa), which use caesium clocks (Fagard 2006).

The two main tasks of the DORIS system are precise orbit determination (POD) of the satellites carrying DORIS and the accurate positioning of the DORIS ground stations. In both cases, this involves comparing the actual DORIS measurements (Doppler count converted into line-of-sight relative velocity) with theoretical values computed from a number of geophysical and technical models describing the station position and the satellite motion. The discrepancies between *measured* and *theoretical* values are called "measurement residuals". In the POD and station positioning processes, the measurement residuals are minimized by the least-squares adjustment of different parameters that reflect our imperfect knowledge of certain aspects of the models.

In particular, at each pass of a DORIS satellite above a DORIS beacon, two parameters are usually adjusted: (1) a zenithal tropospheric delay (MZB, measurement zenithal bias) to account for the uncertainties in the knowledge of the water–vapour content of the troposphere in the vicinity of the beacon, and (2) a frequency bias (MFO, measurement frequency offset) to account for both the transmitter and the receiver frequency offsets with respect to their nominal values (Dorrer et al. 1991).

A possible error in the receiver frequency offset Δf_{SAT} will translate, through the simplified Doppler Eq. (1), into a relative velocity error $\Delta V_{\mathrm{SAT\_BEA}}$ (Eq. 2).

$$V_{\mathrm{SAT\_BEA}} = \frac{c}{f_{\mathrm{BEA}}}\left(f_{\mathrm{BEA}} - f_{\mathrm{SAT}} - \frac{N_{\mathrm{Dop}}}{\Delta t}\right) \tag{1}$$

where V_{SAT_BEA} is the relative velocity between the satellite and the beacon, f_{BEA} and f_{SAT} are the transmitter and receiver frequencies, N_{Dop} is the Doppler count, Δt is the count interval and c is the speed of light.

$$\Rightarrow \Delta V_{SAT\_BEA} = -c\frac{\Delta f_{SAT}}{f_{BEA}} \tag{2}$$

The error in relative velocity is directly proportional to the error in satellite frequency. If the structure of the satellite frequency error is constant over the passage, then solving for one MFO per pass will solve the problem; if it is not, then one would have to consider linear (bias + drift), quadratic or even higher order corrections.

3 Evidence of the instability of the Jason-1 DORIS USO related to the SAA

Besides station positioning, a straightforward way to look at a DORIS receiver frequency evolution is to look at the frequency offsets (MFO) obtained during the passes over the master beacons. The long-term stability of the caesium clocks at the master beacons is greater by a few orders of magnitude than that of the DORIS USOs. As such, one can consider the MFOs obtained during the passes over the master beacons as the satellite's receiver frequency offset at that time, the transmitter frequency offset being negligible. Figure 1 shows the long-term drifts of all the available DORIS receivers, obtained through the use of the MFOs above Toulouse and Kourou. On the *Y*-axis, the receiver frequency offset (in Hz) is plotted with respect to its nominal frequency on the 2 GHz channel, which is the main measurement channel of the DORIS system. The receivers' nominal frequencies are:

- 2.036125 GHz for SPOT-2, SPOT-4, TOPEX/Poseidon and ENVISAT
- 2.03625 GHz for Jason-1 and SPOT-5

The offsets in Fig. 1 can be modelled by simple polynomials, and an exponential term to account for the heating phase at the start-up of the receivers, according to Eq. (3). Equation (3) gives the expression of long-term (LT) frequency offset Δf_{SAT_LT} as a function of t, with t being the date in Julian day since 1950 ($t = 0$ for 01/01/1950 at 00:00 h UT).

$$\begin{aligned}\Delta f_{SAT\_LT}(t) = {} & a_{0_{SAT\_LT}} + a_{1_{SAT\_LT}}(t - t_{0_{SAT\_LT}}) \\ & + a_{2_{SAT\_LT}}(t - t_{0_{SAT\_LT}})^2 \\ & - \exp\left(-\frac{(t - t_{0_{SAT\_LT}}) - a_{3_{SAT\_LT}}}{a_{4_{SAT\_LT}}}\right)\end{aligned} \tag{3}$$

Table 1 gives the parameters $t_{0_{SAT\_LT}}$, $a_{0_{SAT\_LT}}$, $a_{1_{SAT\_LT}}$, $a_{2_{SAT\_LT}}$, $a_{3_{SAT\_LT}}$ and $a_{4_{SAT\_LT}}$ of the long-term fit of the receiver offsets for T/P and Jason-1. The residuals between actual frequency measurements over the master beacons and their long-term fits do not exceed 0.1 Hz for T/P and 0.6 Hz for Jason-1 on the 2 GHz channel, as can be seen in Fig. 2.

The fact that the frequencies of the DORIS receivers drift on the long term does not cause a problem as long as they remain moderate, since those receiver offsets are absorbed by the MFO parameters adjusted at each pass over a DORIS station. The problem occurs when the receiver frequency varies rapidly and greatly within one pass, i.e. within 20 min, which is the average duration of a pass, and could be mistaken with a station position error.

In order to examine this, we have plotted in Fig. 2 the residual DORIS receiver offsets of T/P and Jason-1 above the master beacons of Toulouse and Kourou, once the long-term drifts given by Eq. (3) have been removed.

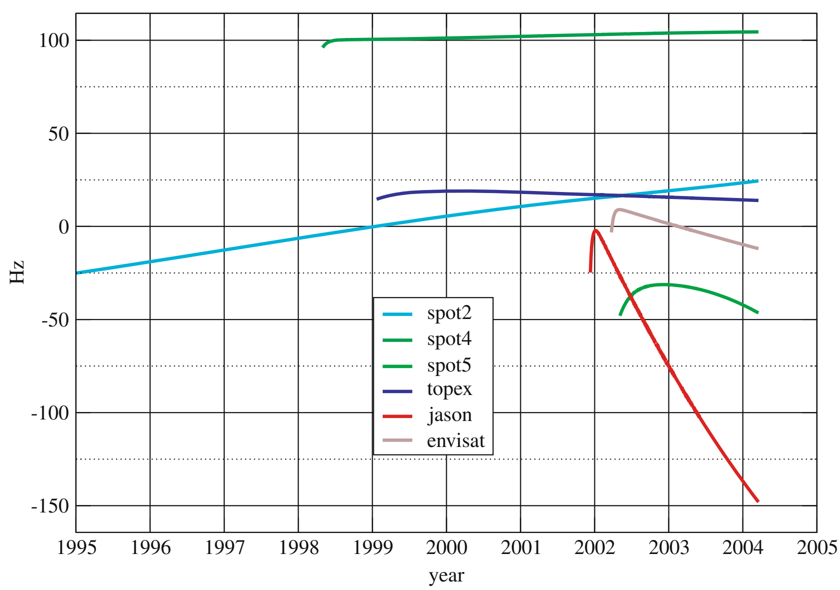

Fig. 1 Measured long-term drifts of the different DORIS on-board oscillators with respect to their nominal frequency

Table 1 Parameters of the long-term fit of T/P and Jason-1 frequency offsets on the 2 GHz channel

	$t0_{SAT\_LT}$	$a0_{SAT\_LT}$	$a1_{SAT\_LT}$	$a2_{SAT\_LT}$	$a3_{SAT\_LT}$	$a4_{SAT\_LT}$
TOPEX/Poseidon	17880	21.3317	−4.20241e-3	2.67452e-7	342.608	163.949
Jason-1	18970	6.81786	−0.234598	6.01552e-5	37.4355	10.9569

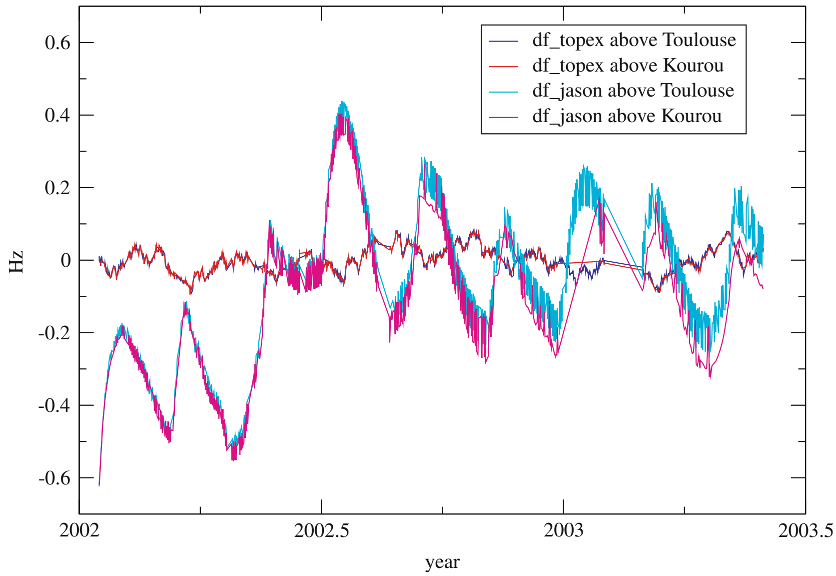

Fig. 2 Residual DORIS receiver frequency offsets for TOPEX/Poseidon and Jason-1 measured above the Toulouse and Kourou master beacons, once the long-term drifts in Fig. 1 have been removed

Several features can be observed in Fig. 2:

- Both satellites display a medium-term oscillation of their frequency (much greater for Jason-1 than for T/P) at the period of 59 days, which is half the period of rotation of their orbital plane with respect to the direction of the Sun.
- The frequency offsets measured above Toulouse and Kourou (dark-blue and red curves in Fig. 2) at a given time are coherent for T/P, while for Jason-1 (light-blue and magenta curves), they are drifting away.
- The discrepancy of the offsets between ascending and descending passes ("thickness" of the curves) is constant and small in the case of T/P, increasing with time in the case of Jason-1.
- More and more points are missing in the magenta (Jason-1) curve, showing that more and more passes above Kourou are lost in the pre-processing. CNES uses a Guier (1963) filter to perform the original screening of the data. It consists in the adjustment, for each pass over a beacon, of a few parameters, representative of an along-track and a radial orbit error with respect to the nominal orbit. The data is then edited according to two criteria: (1) the post-adjustment scatter of the residuals, and (2) the absolute values of the Guier parameters. It is on this last criterion that whole passes are lost above Kourou: since the SAA effect is similar in its results to an error in the station position that can reach a few metres (Willis et al. 2004), the Guier filter interprets this as a large orbit error and suppresses the complete pass.

Figure 3 displays the Jason-1 frequency offsets above three stations (the two master beacons of Kourou and Toulouse, and one standard beacon in the vicinity of the SAA, Ponta Delgada on the island of Sao-Miguel in the Azores) once long- and medium-term trends have been removed (by long- and medium-term, we mean periods ranging from secular to approximately 1 day). The medium-term trends are obtained by smoothing the curves of Fig. 2 with a Vondrak-type low-pass filter (Vondrak and Cepek 2000) with a cut-off period of 0.7 day in the case of T/P and 15 days in the case of Jason-1.

Notice that for all stations in Fig. 3, the ascending and descending passes align along two diverging lines, and that the discrepancy between ascending and descending passes is increasing quasi-linearly with time.

While the passes over Toulouse and Kourou provide accurate observations of the Jason-1 frequency offset at the epoch of the passes, that is to say 4 to 6 times a day, it is insufficient to continuously monitor the offset of Jason-1 frequency.

In the next section, the method is explained that has been devised to overcome this limitation: T/P has been used as a "flying frequency standard", propagating the information on the zenithal biases and frequency offsets of the ground beacons to Jason-1. This method takes advantage of the high stability of T/P frequency on the short-term compared to Jason-1

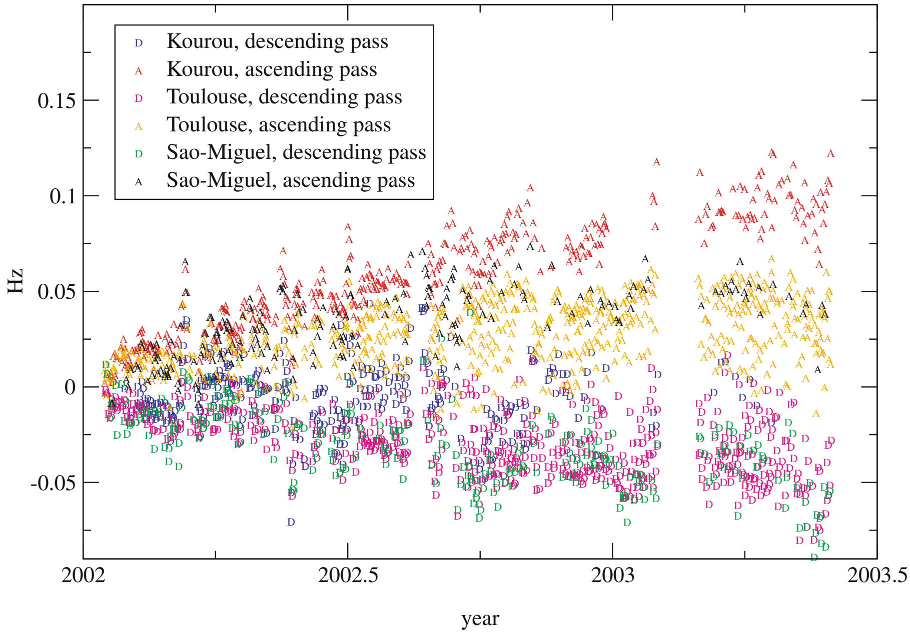

Fig. 3 Jason-1 frequency offsets above three stations (long- and medium-term drifts removed)

(cf. Fig. 2) and on the peculiarity that, during the tandem phase, the two satellites were orbiting very close to each other.

4 Method for observing Jason-1 frequency excursions

Since its launch on December 7, 2001 until August 15, 2002, Jason-1 has been flying in the so-called "tandem phase" (Chelton and Schlax 2003), on the same track as T/P, 60 seconds ahead. Then from August 15, 2002 onward, the two satellites have been flying close to each other on two parallel tracks separated by 150 km maximum. In both cases T/P and Jason-1 have an almost simultaneous visibility of the same DORIS beacons, within a few seconds, and under a similar geometry of observation.

The principle of the method for continuously observing the Jason-1 frequency offset is to "clean" the frequency offsets (MFO) and zenithal biases (MZB) determined by T/P until they are as close as possible to the real parameters of the ground beacons; then use those parameters for the computation of Jason-1 DORIS measurement residuals (using a fixed precise orbit ephemeris); and finally interpret these residuals solely as the signature of the variable frequency offset of Jason-1. The detailed procedure is given below:

1. Compute precise orbits of T/P and Jason-1
2. Save MFO and MZB parameters from T/P and Jason-1; save Jason-1 precise orbit
3. With the MFO parameters of T/P over the master beacons, compute an accurate long- and medium-term evolution of T/P's frequency and remove it from the MFOs; likewise for Jason-1. The T/P's MFOs are now close to the ground beacons' frequency offsets at the epoch of the passes, apart from the errors induced by the T/P's orbit error and by its short-term (10 s to a few hours) frequency instability
4. Using the previously saved Jason-1 orbit, recompute Jason-1 measurement residuals, forcing the MFO and MZB values to those obtained by T/P in step 3
5. Neglecting the errors induced by Jason-1 orbit error, by the aforementioned uncertainties in MFO and MZB and by the time interval separating T/P and Jason-1 passes, the measurement residuals can now be interpreted as an image of Jason-1 frequency fluctuation through the use of the conversion equation:

$$\frac{\Delta f_{\mathrm{SAT}}}{f_{\mathrm{SAT}}} = -\frac{f_{\mathrm{BEA}}}{c * f_{\mathrm{SAT}}} * \text{residual} \tag{4}$$

where f_{SAT} is the nominal receiver (satellite) frequency, f_{BEA} is the nominal transmitter (beacon) frequency, and *residual* is the Doppler residual (in m/s). Equation (4) is deduced from Eqs. (1) and (2). Note that the conversion factor $-f_{\mathrm{BEA}}/c * f_{\mathrm{SAT}}$ only depends on the nominal frequencies f_{BEA} and f_{SAT}, and not on the altitude of the satellite. In the case of Jason-1, since f_{BEA} and f_{SAT} are equal:

$$\frac{\Delta f_{\mathrm{SAT}}}{f_{\mathrm{SAT}}} = -\frac{1}{c} * \text{ residual} \tag{5}$$

Although the sources of uncertainty mentioned earlier introduce noise in the results, this method has been successful, with the noise level remaining at least an order of magnitude below the signal. This method has allowed the almost continuous observation of Jason-1 frequency offset; an example of it is given in Fig. 4 for two different cycles of Jason-1 (Jason-1 cycles last approximately 10 days); and has opened the way to the modelling of Jason-1 oscillator behaviour in response to the influence of the SAA, as explained in Sect. 5. In Fig. 4,

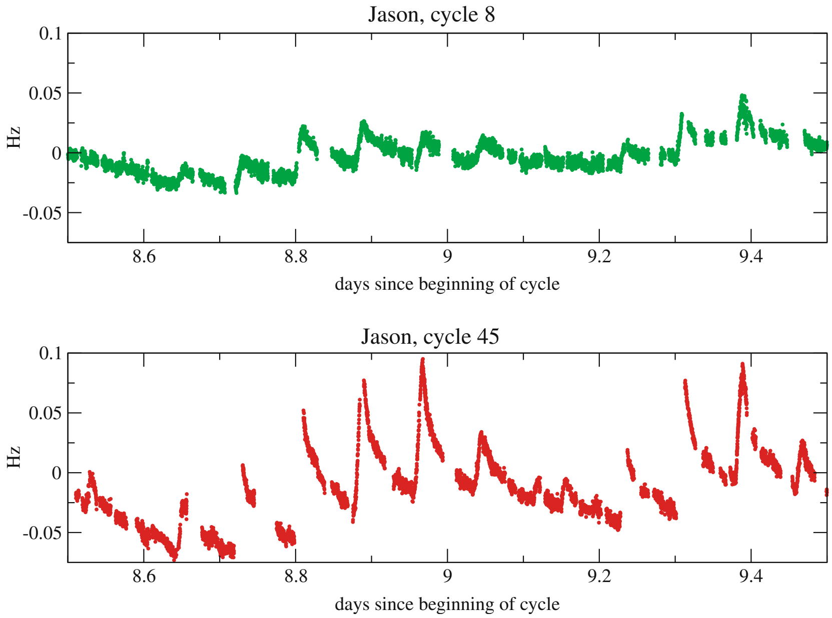

Fig. 4 Jason-1 frequency offsets for part of cycles 8 (2002/03/25–2002/04/04) and 45 (2003/03/27–2003/04/06)

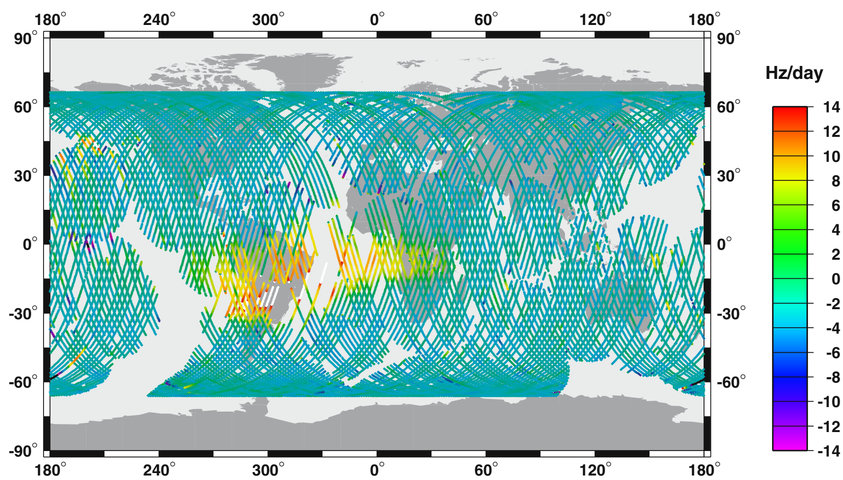

Fig. 5 Geographical plot of the time derivative of Jason-1 frequency offset (Jason-1 frequency change rate) for cycle 26 (2002/09/20–2002/09/30)

the sharp changes in the frequency correspond to the crossing of the SAA area by Jason-1 (approximately 12 times a day). Notice the increase of amplitude of the signal between cycle 8 (2002/03/25 to 2002/04/04) and 45 (2003/03/27 to 2003/04/06).

Plotting the time-derivative of Jason-1 frequency offset on a map, for instance for cycle 26 (2002/09/20 to 2002/09/30), one obtains Fig. 5, where the outline of the SAA is clearly visible and testifies its involvement in Jason-1 frequency excursions.

Thus, T/P and Jason-1 operating simultaneously allow the observation and characterization of Jason-1 USO behaviour. Since T/P's DORIS final failure on November 1, 2004, things have become more difficult, but the observation and modelling of Jason-1's oscillator is still possible through the use of all the other satellites carrying DORIS (SPOT-2, SPOT-4, SPOT-5 and ENVISAT) as replacements for T/P. This will be presented in Sect. 6.2.

5 Modelling the oscillator's response to exposure to high-energy protons

Based on the observation of Jason-1 frequency signal and on the result of technological studies (Canzian 2005), a simple model is proposed for the behaviour of Jason-1 DORIS oscillator. This model involves, on the one hand, the physical source of the perturbations of the DORIS oscillator, in the form of a $1° \times 1°$ map of the SAA at the altitude of Jason-1 (1,300 km), and on the other hand, it involves the response of the oscillator to this excitation, through a set of parameters that can vary with time.

Basically, under exposure to high-energy protons, a quartz oscillator will react by a frequency drift (positive or negative), proportional through an amplitude factor to the level of exposure (the "dose exposure"); by an exponential relaxation behaviour once the exposure is stopped; and by a "memory effect" corresponding to the fact that the frequency does not come back to its initial level, even a long time after the exposure has been stopped. The following set of parameters has therefore been defined:

- A: amplitude factor relating the dose received by the quartz oscillator to the dose exposure
- τ: time constant of the relaxation behaviour
- μ: memory effect coefficient
- dose_exposure: in its present state, a $1^\circ \times 1^\circ$ geographical map of the mean SAA intensity at the altitude of Jason-1

The Jason-1 frequency offset at date t is given by the following formula:

$$\frac{\Delta f_{\mathrm{Jas}}}{f_{\mathrm{Jas}}}(t) = (1-\mu) * \mathrm{current\_dose}(t) + \mu * \mathrm{accumulated\_dose}(t) \quad (6)$$

where current_dose and accumulated_dose at date t are obtained by numerical integration along the orbit of the satellite according to the differential Eq. (7):

$$\frac{d(\mathrm{accumulated\_dose})}{\mathrm{d}t} = \mathrm{dose\_flux}$$
$$\frac{d(\mathrm{current\_dose})}{\mathrm{d}t} = \mathrm{dose\_flux} - \frac{\mathrm{current\_dose}}{\tau} \quad (7)$$

with :

$$\mathrm{dose\_flux} = A * \mathrm{dose\_exposure}$$

In Eq. (7), dose_flux is the dose received by the quartz per unit of time, while $\mathrm{dose\_flux} - \frac{\mathrm{current\_dose}}{\tau}$ represents an effective dose rate. An integration time-step of 10 s was found empirically to be adequate.

Alternatively to Eq. (6), the frequency response of Jason-1 to the SAA could be modelled as:

$$\frac{\Delta f_{\mathrm{Jas}}}{f_{\mathrm{Jas}}}(t) = \alpha * \mathrm{current\_dose}(t) + \beta * \mathrm{accumulated\_dose}(t) \quad (8)$$

with α and β being independent parameters for the current dose and for the accumulated dose, but then there would be no amplitude parameter A (meaning dose_flux=dose_exposure). The two formulations [Eqs. (6) and (8)] are equivalent through the parameter transformations: $\alpha = (1-\mu) * A$ and $\beta = \mu * A$. The alternative formulation in Eq. (8) is mentioned because it can be useful in making a link with technological studies (e.g. Canzian 2005), where the coefficients of the current_dose and the accumulated_dose are determined separately.

We will see in Sect. 6 how the parameters A, τ, μ and *"dose exposure"* have been adjusted. In order to do so, the partial derivatives of $\Delta f_{\mathrm{Jas}}/f_{\mathrm{Jas}}$ with respect to the parameters have had to be numerically integrated, simultaneously with the numerical integration of current_dose and accumulated_dose themselves.

6 Models for Jason-1 DORIS USO n°2 and n°1

6.1 Model for Jason-1 DORIS USO n°2

From January 15, 2002 until June 25, 2004, covering Jason-1 cycles 1 to 90, the redundant DORIS USO (USO n°2) was ON aboard Jason-1. Most available cycles over that period (cycles 1 to 71) have been used in order to obtain the model for USO n°2. The parameters that are solved-for are A, τ and μ (one set for each cycle) and a map of the SAA "*dose exposure*" (one for the whole 2002–2004 period).

The determination of these parameters has been an iterative process, the first step of the process being to ascertain that the hypothesis of a stable SAA "*dose exposure*", stable in position and extent over the whole period, was a valid one. For this purpose, the SAA "*dose exposure*" has been first modelled geographically as a simple bi-dimensional Gaussian function, instead of a $1^\circ \times 1^\circ$ grid:

$$\mathrm{dose\_exposure} = \exp\left(-\frac{1}{2}\left(\frac{\mathrm{lat}-\mathrm{lat}_{\mathrm{SAA}}}{\mathrm{SAA\_lat\_extent}}\right)^2\right) * \exp\left(-\frac{1}{2}\left(\frac{\mathrm{lon}-\mathrm{lon}_{\mathrm{SAA}}}{\mathrm{SAA\_lon\_extent}}\right)^2\right) \quad (9)$$

where $\mathrm{lat}_{\mathrm{SAA}}$ is the latitude of the centre of the SAA area, $\mathrm{lon}_{\mathrm{SAA}}$ is the longitude of the centre of the SAA area, SAA_lat_extent is the latitudinal extent of the SAA area, and SAA_lon_extent is the longitudinal extent of the SAA area.

The parameters of the Gaussian function have been determined for 17 cycles (Fig. 6). The average uncertainty of the parameters (not shown in Fig. 6) is 0.6° for $\mathrm{lat}_{\mathrm{SAA}}$ and SAA_lat_extent and 2° for $\mathrm{lon}_{\mathrm{SAA}}$ and SAA_lon_extent. Compared to constant mean values, the solution variations remain within those error bars and validate the hypothesis of a stable SAA "*dose exposure*".

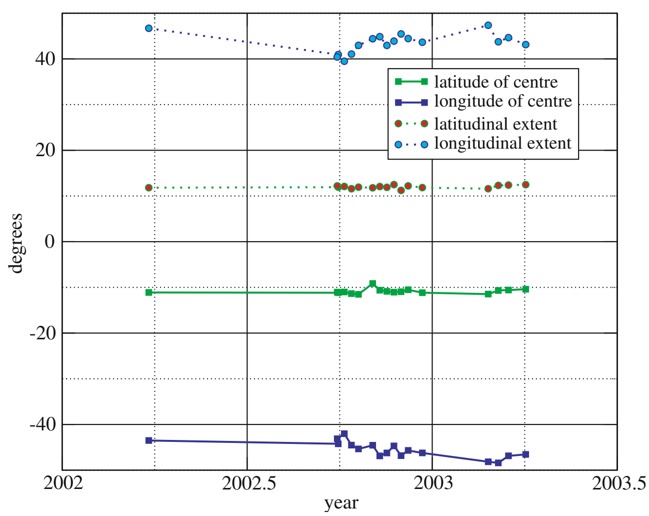

Fig. 6 Time-evolution of the SAA centre location and SAA geographical extent

It was then possible to derive, through the least-squares adjustment of all the other parameters, the mean $1^\circ \times 1^\circ$ grid values of the SAA (at the altitude of Jason-1) and the time-evolution of A, τ and μ. The results are a novel image of the dose density of the SAA at 1,300 km altitude and a model of the response of DORIS USO n°2 to the SAA, which will be described subsequently.

6.1.1 $1^\circ \times 1^\circ$ *grid of the SAA at the altitude of Jason-1*

Obtaining directly by inversion a $1^\circ \times 1^\circ$ grid of the SAA at the altitude of Jason-1 was not advisable for three reasons:

- The number of parameters involved: approximately 44,000;
- The coarse spacing of T/P & Jason-1 tracks (315 km at the equator), resulting in a weak number of measurements per square degree and an unstable determination of some grid nodes,
- The necessity to smooth the solution in order to filter out short-wavelength errors.

The SAA map was therefore determined on a $2^\circ \times 2^\circ$ grid (approximately 11,000 parameters). This grid was converted to spherical harmonics, limiting the expansion to degree 60, and converted back to grid points, with a 1° spacing in order to allow a precise interpolation of the grid by users. The result is shown in Fig. 7.

The "dose exposure" grid in Fig. 7 is in dimensionless units. Multiplied by $A(t)$, it gives an upper bound of the drift rate of Jason-1 frequency on the 2 GHz channel, at any date t and at any location on the globe. There is no way, with Jason-1 solely, to have access to the absolute value of the dose exposure, in rad/h for instance, because there is no instrument aboard Jason-1 that could help establish the calibration factor of the grid in Fig. 7. This grid can then be interpreted only in a relative way. Since the mean value of the grid and the mean value of the A parameter are one-to-one correlated, an additional condition had to be imposed in order to enable solving for both the grid and the A parameter. This arbitrary condition was that the grid maximum value be 1.5.

Hopefully, the Carmen instrument (a radiation-meter) scheduled to be onboard the future Jason-2 satellite (due for launch in 2008) will allow establishment of an absolute calibration of Fig. 7.

The outline of the SAA in Fig. 7 is similar to the one observed by the South Atlantic Anomaly Detector (SAAD, Fig. 8) and Multi-angle Imaging SpectroRadiometer (MISR, Fig. 9) instruments on-board the ROSAT (Roentgen SATellite) and Terra satellites, or by the Medium Energy Proton

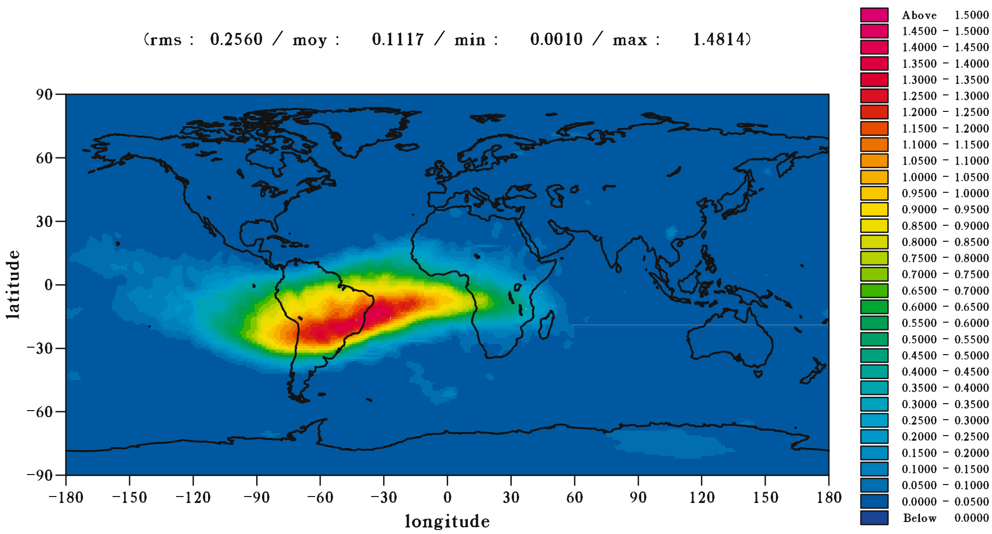

Fig. 7 Plot of the relative SAA dose exposure in 2002–2005 at the 1,300 km altitude of Jason-1 (dimensionless units)

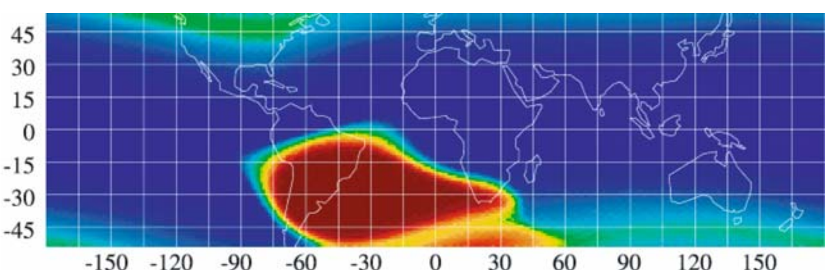

Fig. 8 Picture of the relative location of the SAA in 1996 at 580 km from ROSAT (courtesy of NASA)

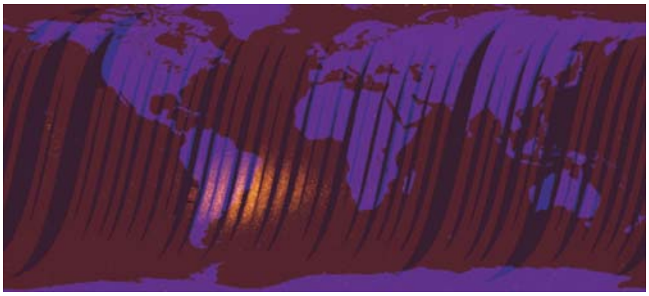

Fig. 9 Image of the SAA captured by the MISR instrument on-board NASA's Terra spacecraft in February 2000 at 705 km (image courtesy of MISR instrument team, NASA)

and Electron Detector (MEPED) particle sensors (Fig. 10) on-board the NOAA POES (Polar Orbiting Environmental Satellites) satellites.

The ROSAT satellite (altitude 580 km, inclination 53°) was a German/US/UK X-ray observatory operating between 1990 and 1999; it carried the SAAD. The MISR instrument onboard NASA's Terra spacecraft (altitude 705 km, inclination 90°) was able, just after its launch in Feb 2000, when its cover was still closed, to take an image of the SAA thanks to the sensitivity of its cameras to energetic protons (Diner et al. 1998, 2002). The MEPED instrument (Huston and Pfitzer 1998) is onboard the NOAA's POES satellite (altitude 833 km, inclination 90°).

In Fig. 8, the image of the SAA from the SAAD differs noticeably from the new image of the SAA obtained by the present study (Fig. 7), in position, extent and shape. This is partly attributable to the important difference in altitude of the maps (580 km vs 1,330 km), to the time separating the two images (8 years) and possibly to the level of energy measured by the SAAD and DORIS. Figure 7 is more similar to Figs. 9 and 10.

Compared to the images from the MEPED proton sensors in the bands 16–70 and 140–275 MeV, the new image of the SAA in Fig. 7 is stretched in longitude. This is coherent with the higher altitude of Jason-1: the intersection of a sphere of greater radius with the torus of the Van Allen belts is more oblate. It also shows a slight difference of the SAA location in the north-east, particularly in its eastern extent, which is shifted from Namibia to the Gulf of Guinea.

6.1.2 *Model parameters for Jason-1 DORIS USO n°2*

Figure 11 displays the time-evolution of the model parameters for DORIS USO n°2.

As can be seen in Fig. 11, the state of DORIS USO n°2 is clearly worsening over time:

- The memory effect μ and time constant τ decrease strongly; μ from 53 to 10%, τ from 16 to 7 min;
- The amplitude factor A increases quasi-linearly from 5 to 36. Converted to Hz/day through the multiplication by the "*dose exposure*" grid (it must be kept in mind that the A parameter has no meaning without its associated "*dose exposure*" grid), a factor 36 represents, where the maximum "*dose exposure*" coefficient is 1.48, a drift of more than 50 Hz/day on the 2 GHz band at the centre of the SAA. This corresponds to a relative frequency rate $\frac{d(\Delta f_{SAT}/f_{SAT})}{dt}$ of 2.5×10^{-8} per day, more than one order of magnitude greater than the specifications (5×10^{-10} per day, reduced to 1.5×10^{-10} per day for the last generation of instruments, cf. Candelier et al. 2003) for the medium-term stability of the DORIS instruments over a pass of 10 min.

The USO n°2 oscillator behaves as if it was more and more permeable to the protons: receiving steadily more dose for the same exposure, but letting it decay faster and retaining less of it (memory) on the long term. In this respect, the change of USO at the end of cycle 91, in June 2004, proved to be an appropriate decision.

Because some cycles have a high noise level, and in order to obtain a model that can be predictive, the final model for DORIS USO n°2 consists in a series of polynomial or exponential expansions for parameters A, τ and μ: Eqs. (10), (11), (12). They are represented by the blue, dark green and red curves in Fig. 11.

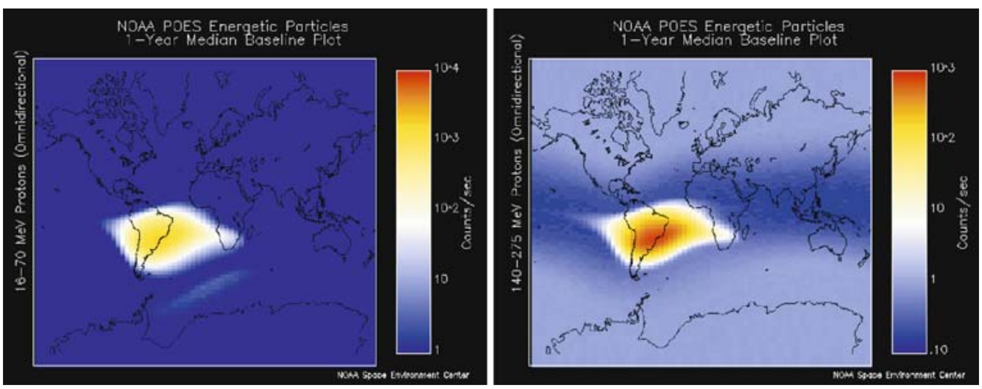

Fig. 10 Images of the MEPED proton sensors in the 16–70 and 140–275 MeV bands in 2005 at 833 km (images courtesy of NOAA Space Environment Centre)

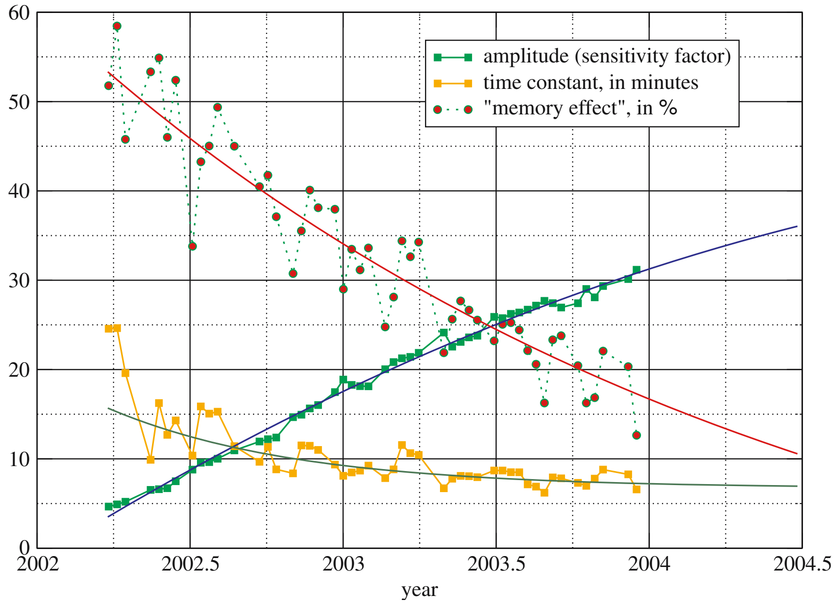

Fig. 11 Time-evolution of the model parameters for DORIS USO no. 2

In the following equations, t is the time in Julian days since the start of 1950; $t_0 = 19000$ (January 8, 2002) is the reference date.

Temporal evolution of the amplitude (order two polynomial):

$A(t) = a0_{\text{amp}} + a1_{\text{amp}}(t - t_0) + a2_{\text{amp}}(t - t_0)^2$

with:

$$\begin{cases} a0_{\text{amp}} = -0.892 \\ a1_{\text{amp}} = 5.846\text{e} - 2 \\ a2_{\text{amp}} = -1.936\text{e} - 5 \end{cases} \quad (10)$$

Temporal evolution of the relaxation time (exponential decay):

$\tau(t) = a0_\tau + a1_\tau \exp\left(-\frac{t - t_0}{a2_\tau}\right)$

with:

$$\begin{cases} a0_\tau = 4.67\text{e} - 3 \\ a1_\tau = 8.8\text{e} - 3 \\ a2_\tau = 222.39 \end{cases} \quad (11)$$

Temporal evolution of the memory effect (exponential decay):

$\mu(t) = a0_{\text{me}} + a1_{\text{me}} \exp\left(-\frac{t - t_0}{a2_{\text{me}}}\right)$

with:

$$\begin{cases} a0_{\text{me}} = -0.16755 \\ a1_{\text{me}} = 0.76542 \\ a2_{\text{me}} = 873.69 \end{cases} \quad (12)$$

The final step is to use the parameters that have been obtained in order to compute the modelled values of Jason-1 frequency offsets. As mentioned before, this requires the integration of Eq. (7) along the orbit of the satellite, taking into account the variation of the model parameters with time. An example in April 2003 of the result of such modelling is shown in Fig. 12, where the black dots are the pseudo-observations obtained by the method of Sect. 4, and the red line is the modelled offset of Jason-1 USO n°2.

The agreement of the modelled values with the observed values in Fig. 12 is obvious. The modelled values provide a continuous information on the instantaneous frequency offset of Jason-1.

6.2 Model for Jason-1 DORIS USO n°1

Since June 29, 2004, the DORIS USO n°1 has been in operation. For the first 4 months of this period, T/P was available for the determination of the frequency offsets of Jason-1. Since the final failure of the T/P's DORIS receiver on November 1, 2004, the use of T/P has been replaced by the use of all the other satellites carrying DORIS (SPOT-2, SPOT-4, SPOT-5 and ENVISAT) in order to compute the MFO and MZB parameters of the stations.

Although more complex in implementation, since it involves the orbit computation of four satellites and the combination of their station parameter solutions, this new scheme has proved satisfactory and equally precise as using T/P. There is a good agreement between the troposphere and beacon frequency offsets computed from T/P and those computed from the other satellites carrying DORIS; and they both provide, with a difference not exceeding 2%, the same solution for the model parameters of Jason-1 (the agreement was verified for the 4 months when T/P was available for the correction of USO n°1).

Figure 13 gives an example of the Jason-1 computed offsets for USO n°1 in November 2004.

The DORIS USO n°1 obviously differs from instrument n°2: firstly, the influence of the SAA produces a *negative*

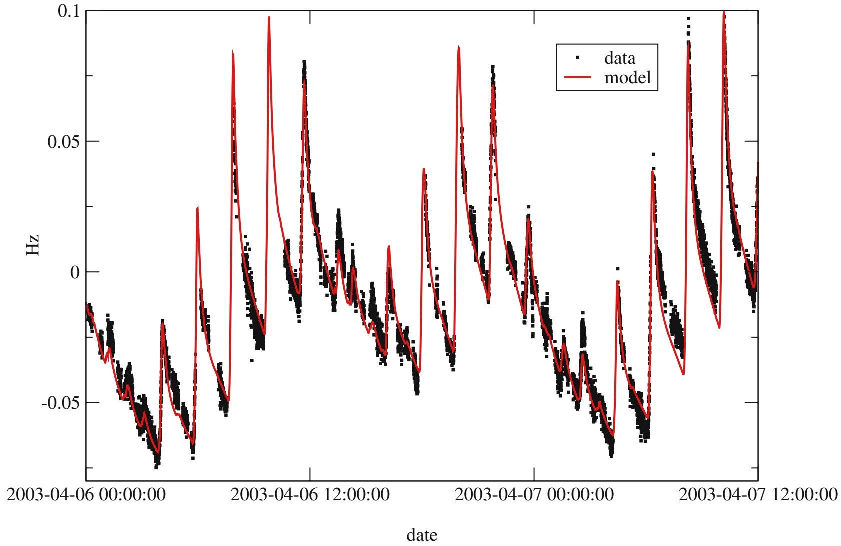

Fig. 12 Jason-1 observed (black) and modelled (red) frequency offsets of DORIS USO no. 2. (zoom on cycle 55)

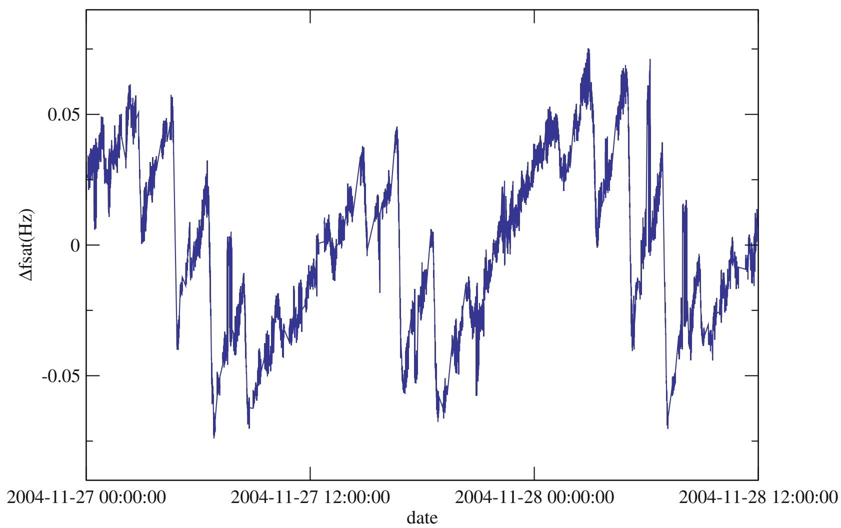

Fig. 13 Example of Jason-1 DORIS USO no. 1. frequency offsets in November 2004

offset instead of a *positive* one; secondly, the relaxation time τ is much longer for USO n°1, and consequently becomes very difficult to decorrelate from the memory effect μ. The approximate value that was estimated for τ is 120 min, longer than one orbital revolution which, according to technological studies (Canzian 2005 and P. Escudier, personal communication) is hardly realistic. Taking into account the above considerations and the difficult decorrelation between τ and μ, it was decided to set τ to a value of 40 min and remove it from the parameter list.

The parameters of the model for USO n°1 are therefore quite different from the ones of USO n°2, as can be seen in Fig. 14: all parameters are more or less constant in time and the level of the amplitude A (negative in this case) remains low (-8 to -11), compared to USO n°2 ($+5$ to $+36$).

There is a modulation of the parameters at the periods 59 and 118 days (Fig. 14), correlated with the rotation of the orbital plane of Jason-1 with respect to the direction of the Sun (of period 118 days). The modulation at 59 days amounts to 4% of the total power, while the one at 118 days amounts to 2.5% of it. This modulation was already present in the parameters of the USO n°2. For the sake of simplicity and reliability however, the time-evolution of the A parameter is modelled by a linear function: Eq. (13) (the red line in Fig. 14), and the μ parameter is modelled as a constant: $\mu = 0.7$ (the green line in Fig. 14).

$$A = -8.4345 - 0.00389 * (\text{date} - 19,900) \tag{13}$$

with date in Julian days since the start of 1950.

Finally, the use of this new model for DORIS USO n°1 allows, as in the case of USO n°2, the computation of the modelled values of Jason-1 frequency offset. Figure 15 gives an example of the modelling of Jason-1 USO n°1 in December 2004.

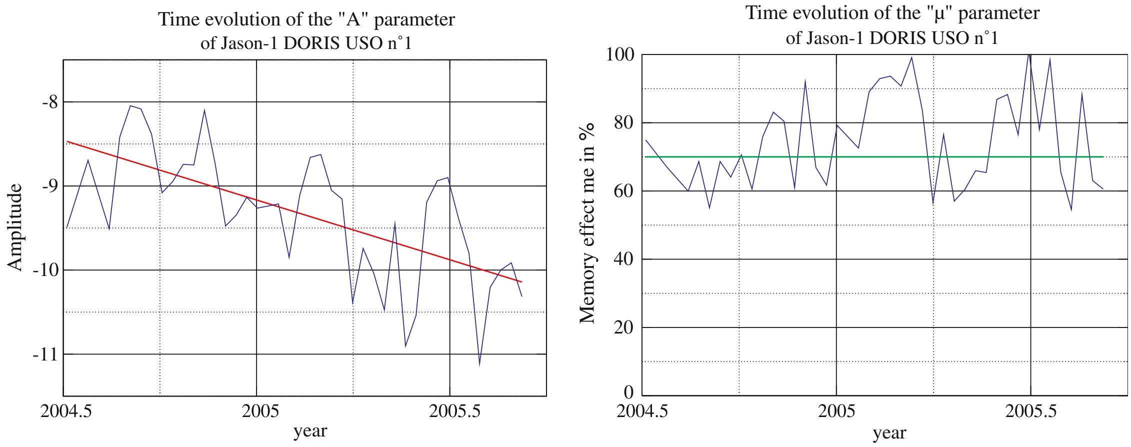

Fig. 14 Time-evolution of the model parameters for DORIS USO no. 1

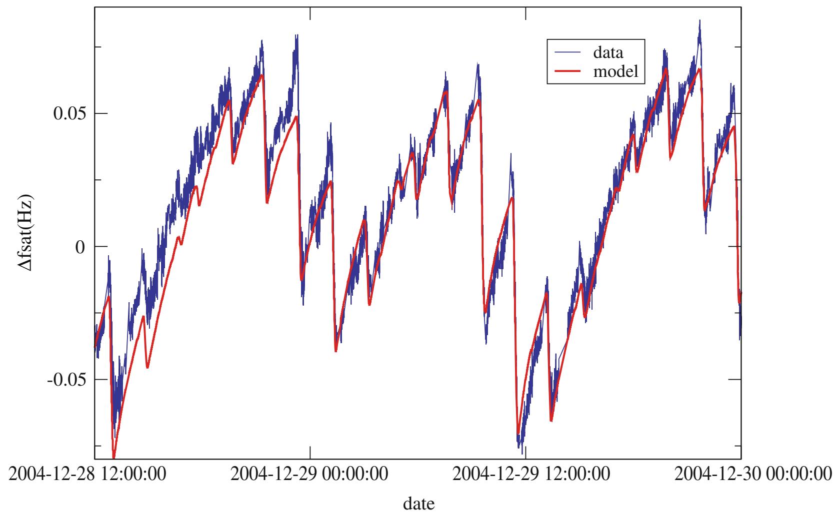

Fig. 15 Jason-1 observed (*blue*) and modelled (*red*) frequency offsets of DORIS USO no. 1 (zoom on cycle 109)

As for Figure 12, the agreement in Fig. 15 of the modelled values with the observed values is clear. In this example, there is a period during the first 8 hours when the two signals depart. This type of medium-term error of the model has little consequence on the quality of the correction of the DORIS data since only the rate of change of the frequency has an impact on the measurements. Thus, only short-term variations are important; all long- and medium-term effects are absorbed by the adjustment of the MFOs.

7 Assessing the impact of the model corrections to Jason-1 DORIS data

The impact of the model corrections to Jason-1 DORIS data can be assessed by many different aspects: residuals reduction, quality of the positioning of the stations using Jason-1 alone or Jason-1 together with the other DORIS satellites, reduction of the number of edited DORIS measurements and finally quality of the Jason-1 computed orbits.

Figure 16 shows an example of DORIS performances without and with SAA model corrections for nine 3.5-day orbit arcs of Jason-1 in October 2003. The average reduction of the DORIS measurement residuals, using the SAA model corrections, is of the order of 7%: from 0.375 to 0.350 mm/s for 3.5-day orbit arcs (left plot of Fig. 16). This reduction in measurement residuals is accompanied by a reduction of the number of measurements edited on a three-sigma criterion: an average of 300 DORIS measurements (from 28000) are saved from rejection by the use of SAA model corrections (middle plot of Fig. 16).

Those DORIS-only orbits can be evaluated in terms of orbit accuracy using strongly down-weighted SLR measurements together with the DORIS measurements. Here, the SLR measurements serve only to assess the accuracy of the DORIS orbit (i.e. they are not used in a combined orbit). An improvement of a few millimetres of the SLR residuals

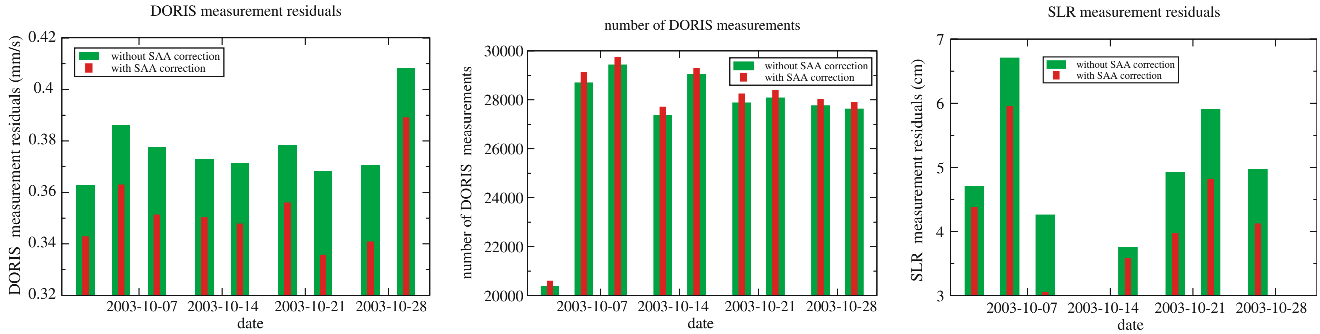

Fig. 16 Jason-1 DORIS measurements without (*green*) and with (*red*) SAA model corrections

Table 2 Comparison of DORIS+SLR orbits (with and without SAA correction) with GPS+SLR orbits for Jason-1 cycles 42–44

	Average bias (cm)			Average rms (cm)		
	Radial	Normal	Tangential	Normal	Radial	Tangential
DORIS without SAA correction	0.0	0.0	0.3	0.5	2.2	1.8
DORIS with SAA correction	0.0	−0.9	0.7	0.4	2.1	1.6

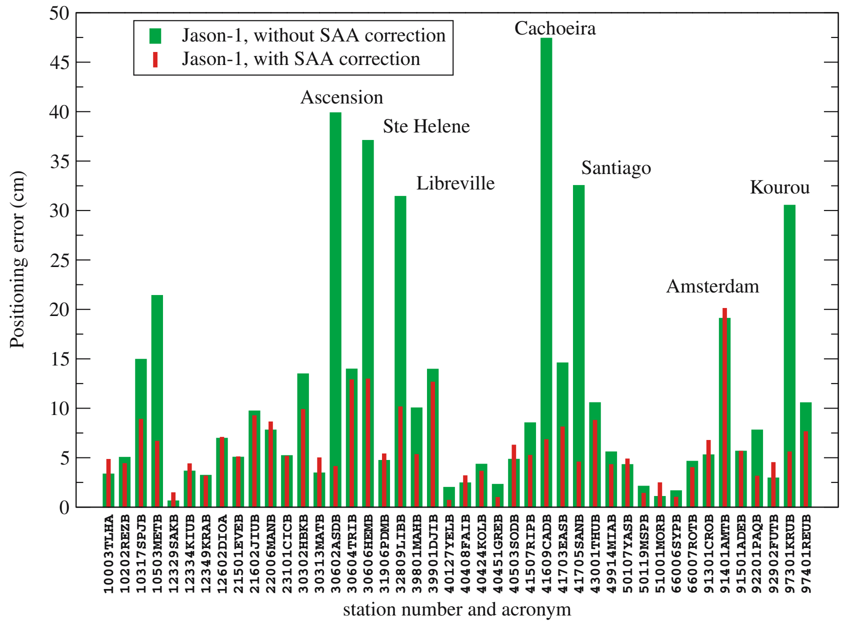

Fig. 17 Comparison between a Jason-1 monthly network solution (June 2005) and the ITRF2000*

is achieved in that case, showing an improvement of the DORIS-only orbit accuracy (right plot of Fig. 16).

However, when the SLR data is not down-weighted and participates in the orbit adjustment, the DORIS SAA correction models bring little in terms of orbit accuracy. Indeed, the quality of the DORIS+SLR orbit is very robust, with or without SAA correction, due to the large redundancy of the DORIS system in terms of number and distribution of the stations and to the accurate positioning of the satellite brought by the SLR.

The SAA perturbations, limited to a small number of stations, are not sufficient to noticeably perturb the orbit of Jason-1 when the SLR data is there to periodically readjust the orbit. As an example, Table 2 presents the comparison of DORIS+SLR orbits (with and without SAA correction) with GPS+SLR orbits for three Jason-1 cycles (42, 43 and 44) in March 2003. There is a slight improvement of the RMS (root mean square) of the comparison in all three directions, although hardly significant.

The last part of this section is devoted to station positioning using Jason-1 data. Figure 17 displays the comparison between the ITRF2000* and a DORIS network solution obtained with Jason-1 alone on the month of June 2005. ITRF2000* is the ITRF2000, extended to include the new stations (i.e. more recent than 2001) that did not appear in ITRF2000. The coordinates of these new stations are

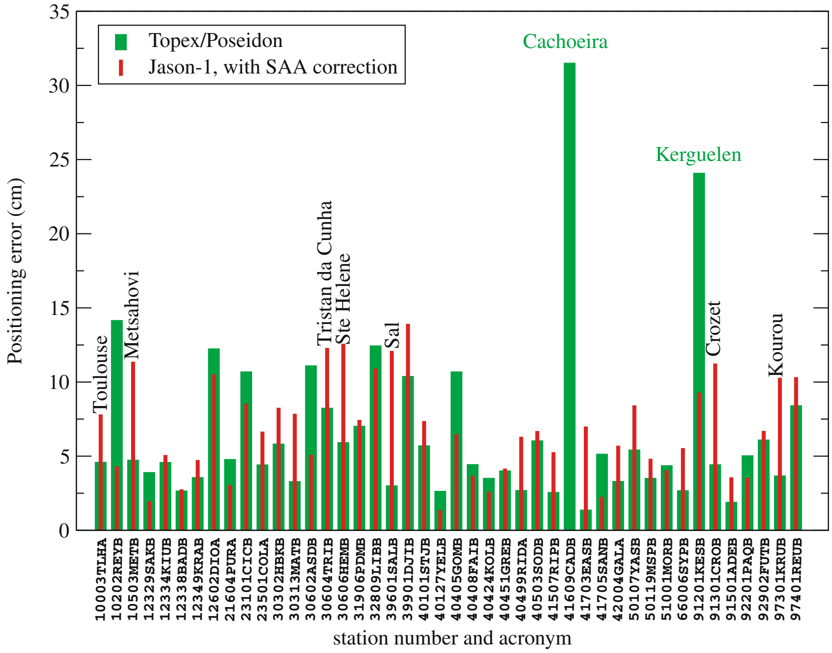

Fig. 18 Comparison between the ITRF2000* and a monthly network solution (September 2004) from T/P and from Jason-1

provided by the IDS in the "DORIS mails". They generally come from reliable geodetic ties with older DORIS sites or with SLR or GPS markers.

In Fig. 17, the green bars give the positioning discrepancy when the SAA is not corrected for and the red bars when it is. Using the SAA correction, the average discrepancy of the station network decreases from 11.3 to 6.1 cm, the major improvements being for the SAA area stations: Ascension island (South Atlantic Ocean), St-Helena island (South Atlantic Ocean), Kourou, Libreville (Gabon), Santiago (Chile) and Cachoeira (Brazil) are where the improvement in station positioning is significant (decreasing from 47 cm to 7 cm). The poor results at Amsterdam island (Indian Ocean) are not assignable to the SAA, but to an accidental antenna instability (Willis and Ries 2005).

The quality of station positioning with Jason-1 is now almost comparable with the one obtained by T/P. Figure 18 displays the discrepancies to ITRF2000* of two T/P and Jason-1 monthly solutions. The quality of positioning is comparable, except for some stations in the SAA vicinity: Toulouse, Metsahovi (Finland), Tristan da Cunha (South Atlantic Ocean), St-Helena, Sal (Cape Verde), Crozet (South Indian Ocean) and Kourou.

Consequently, multi-satellite solutions including Jason-1 are now possible. Figure 19 shows the comparison with the ITRF2000* of multi-satellite (SPOT-2, -4, -5 and ENVISAT) solutions not including Jason-1 (green bars) and including Jason-1 with its SAA correction (red bars). The solution is better with Jason-1 in most cases, 37 cases upon 52 (not considering Jiufeng in China and Amsterdam island, which are problematic stations; Jiufeng because of its lack of data on the early measurements of this station and Amsterdam because of the instability of the antenna plate).

With the SAA corrections, the DORIS data on Jason-1 can now be used in conjunction with the data from the other DORIS satellites and provide multi-satellite solutions that are better than the ones not incorporating Jason-1. This was not the case before, where the inclusion of Jason-1 data would degrade the quality of the network solutions.

8 Discussion and conclusions

A technique has been devised to have access to the continuous observation of Jason-1 frequency excursions due to the SAA. This has allowed the construction of a model of the response of the Jason-1 DORIS USO n°1 and USO n°2 to the SAA. This model was built using almost all of the past observations of Jason-1 frequency offsets, but it can be predictive and therefore serve to correct future observations.

The use of this model allows a reduction of the DORIS residuals, of the number of outlier measurements, an improvement of the DORIS-only orbits but no (or very little) improvement of the DORIS+SLR orbits. Its major impact is on the quality of the DORIS stations positioning. An improvement is observed for most stations, but particularly for those in the SAA area. This allows re-incorporating Jason-1 in the determination of the DORIS station network, when it previously had to be excluded because it was contributing more noise than information to the solution.

A by-product of this study is a new map of the SAA at the 1,300 km altitude of Jason-1. The calibration of this map is for the moment relative, rather than absolute, and one has to wait for the Carmen instrument on-board Jason-2 to obtain an absolute calibration. Jason-2 ought to be much less affected

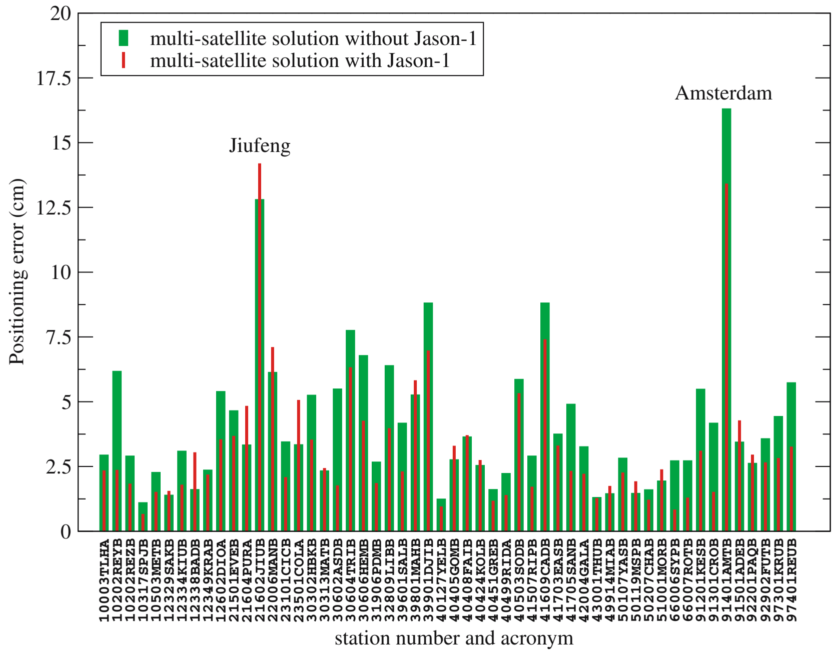

Fig. 19 Comparison between a multi-satellite monthly network solution with/without Jason-1 (June 2005) and the ITRF2000*

by the SAA than Jason-1 because, after years of research, the oscillator problem on Jason-1 has now been identified.

Contrarily to all the other quartz oscillators of the DORIS USOs, the ones of Jason-1 had not been hardened against the radiations by preventive submission to a high level of irradiation (5 to 50 krad). Canzian (2005) shows that a pre-irradiation of 5 krad is sufficient to efficiently reduce the sensitivity of the quartz resonators to the low level of radiations, of the order of 1 rad/h, found at the altitude of Jason-1. The defect of Jason-1, which has turned its USO into an SAA detector, has been corrected for Jason-2.

In a general manner, it is important to stress that the Jason-1 problem relative to the SAA is critical for geodetic applications, in particular reference frame determination, but seems far less critical for POD applications (relying more on global models than on the measurements themselves). As discussed in Choi et al. (2004), for POD applications, a simple down-weighting of the DORIS stations in the SAA area might be sufficient, since we have seen in Table 2 the robustness of orbits computed with mixed tracking systems (DORIS + SLR in that case, but the result would probably have been the same for DORIS + GPS or DORIS + GPS + SLR).

However, if it is station positioning we are interested in, then down-weighting is not the solution. Another solution would be to increase the number of parameters solved-for per pass. As explained at the end of Sect. 2, if the satellite frequency offset is not constant over a pass, one may think of solving for linear or even quadratic terms, for the stations in the SAA area. This is simple and efficient, but comes up against a number of objections:

- An increase in the number of parameters results in a weakening of the robustness of the solution, through the increase in the number of degrees of freedom; whereas the SAA model allows avoiding the introduction of additional parameters.
- At certain periods in Jason's life (particularly since 2003), the number of stations affected by the problem spreads far beyond the sole region of the SAA because of the relaxation effect, which is proper to the DORIS USO and not to the SAA extent. Consequently one has to solve for two or even three parameters per pass for a number of stations much greater than strictly the ones of the SAA area.
- In the zones where the SAA effect is the strongest (Kourou, Arequipa, Cachoeira, Ascension, Libreville), a linear drift is not sufficient to account for the frequency variations during one pass. For these stations, a quadratic parameterization would be necessary, increasing the number of parameters and weakening the strength of the solution.

However, as shown in Fig. 18, the actual SAA model is still weaker in the SAA area for some stations than for others. One goal for future developments of the model would be to attain a quality of station positioning with Jason-1, for the stations of the SAA area, that is identical to that of the other stations.

Among the different developments that could be undertaken to improve the present study are:

- A new check of the stability of the SAA map. This could be done by splitting in two the available observations of Jason-1 frequency offsets and determining a SAA map for each subset, in order to compare them and detect a possible temporal evolution.
- Introduce temporal variations in the model parameters (A, τ and μ) at periods of 59 and 118 days so that the

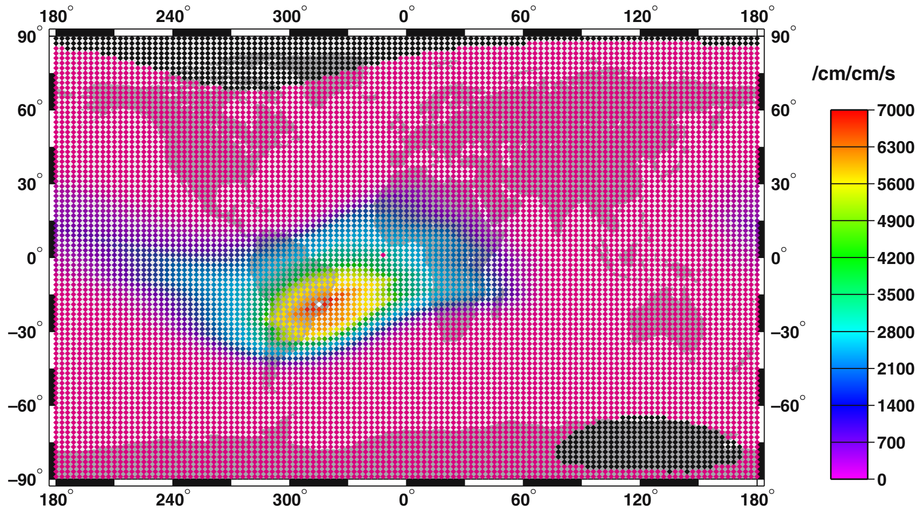

Fig. 20 World map of integral proton flux > 100 MeV at 1,300 km altitude from the AP-8 model (for solar minimum)

modelled parameters more closely follow the per-cycle determined parameters.
- Compare with trapped particle flux models. Apart from comparison to "observational data" (Figs. 8, 9, 10), the SAA grid obtained in this study should be compared to trapped proton flux models. It might lead to an indication on the level of energy of the protons that perturb Jason-1. As an example, on Fig. 20 is plotted the AP-8 MIN integral proton flux > 100 MeV at Jason-1 altitude (1,300 km) from the AP-8 model (Sawyer and Vette 1976; Vette 1991). The similarity with Fig. 7 is striking. Comparison to other models, like CRRESPRO (Meffert and Gussenhoven 1994) for instance, remains to be done.

The SAA correction model, the SAA grid and the associated technical memorandum can be retrieved freely from the IDS Central Bureau ftp site at the address ftp://ftp.cls.fr/pub/ids/satellites/CORRECTIVE_MODEL_JASON1

Acknowledgements This research was supported by CNES. We thank Dr Pascal Willis for providing us with a set of Jason-1 frequency offsets determined by him that have been used for comparison with our own determined frequency offsets. We thank the SPENVIS team for the availability of the trapped radiation models. We also thank Dr Sean Bruinsma and other reviewers for their helpful suggestions on the manuscript.

References

Altamimi Z, Sillard P, Boucher C (2002) ITRF2000, A new release of the International Terrestrial Reference Frame for earth science applications. J Geophys Res 107(B10):2214. DOI 10.1029/2001JB000561

Armstrong TW, Colborn BL (1992) Predictions of induced radioactivity for spacecraft in low Earth orbit. Rad Meas 20(1):101–130

Badhwar GD, Kushin VV, Akatov YA, Myltseva VA (1999) Effects of trapped proton flux anisotropy on dose rates in low Earth orbit. Nucl Tracks Rad Meas 30(3):415–426

Candelier V, Canzian P, Lamboley J, Brunet M, Santarelli G (2003) Space qualified 5 MHz ultra stable oscillators. In: Proceedings of the 2003 IEEE international frequency control symposium, pp 575–582. DOI 10.1109/FREQ.2003.1275155

Canzian P (2005) Rapport de mesures de caractérisation d'oscillateurs sous radiations à faible débit de dose. C-MAC/ONERA/DERTS report 092975_01-C-MAC

Chelton DB, Schlax MG (2003) The accuracies of smoothed sea surface height fields constructed from tandem satellite altimeter datasets. J Atmos Oceanic Technol 20(9):1276–1302. DOI 10.1175/1520–0426(2003)020< 1276:TAOSSS> 2.0.CO;2

Choi KR, Ries JC, Tapley BD (2004) Jason-1 precision orbit determination by combining SLR and DORIS with GPS tracking data. Mar Geod 27(1–2):319–333 DOI 10.1080/01490410490465652

Debaisieux A, Aubry JP, Brunet M (1986) A satellite oscillator for very precise orbitography – the DORIS program. IEEE Trans Ultrason Ferroelectr Freq Control 33(1):121–121

Diner DJ, Beckert JC, Reilly TH, Bruegge CJ, Conel JE, Kahn RA, Martonchik JV, Ackerman TP, Davies R, Gerstl SAW, Gordon HR, Muller JP, Myneni RB, Sellers PJ, Pinty B, Verstraete MM (1998) Multi-angle imaging spectroRadiometer (MISR), instrument description and experiment overview. IEEE Trans Geosci Remote Sens 36(4):1072–1087

Diner DJ, Beckert JC, Bothwell GW, Rodriguez JI (2002) Performance of the MISR instrument during its first 20 months in Earth orbit. IEEE Trans Geosci Remote Sens 40(7):1449–1466 DOI 10.1109/TGRS.2002.801584

Dorrer M, Laborde B, Deschamp P (1991) DORIS (Doppler Orbitography and Radiopositioning Integrated by Satellite). System assessment results with DORIS on SPOT2. Acta Astronaut 25:497–504

Fagard H (2006) 20 years of evolution for the DORIS permanent network: from its initial deployment to its renovation. J Geod (submitted)

Fraser-Smith AC (1987) Centered and eccentric geomagnetic dipoles and their poles, 1600–1985. Rev Geophys 25:1–16

Fu LL, Christensen EJ, Yamarone CA, Lefebvre M, Ménard Y, Dorrer M, Escudier P (1994) TOPEX/Poseidon mission overview. J Geophys Res 99(C12):24369–24381

Guier WH (1963) Studies on Doppler residuals 1: Dependence on satellite orbit error and station position error. JHU/APL TG-503, Applied Physic Laboratory, The Johns Hopkins University, Laurel

Heynderickx D (1996) Comparison between methods to compensate for the secular motion of the South AtlanticAnomaly. Nucl Tracks Radiat Meas 26:325–331

Huston SL, Pfitzer KA (1998) Space environment effects: low-altitude trapped radiation model. NASA/CR-1998–208593, NASA′s Space Environments and Effects (SEE), NASA Marshall Space Flight Centre, AL 35812, pp 63

Meffert JD, Gussenhoven MS (1994) CRRESPRO documentation, PL-TR-94–2218, Environmental Research Papers, 1158, Phillips Laboratory

Ménard Y, Fu LL, Escudier P, Parisot F, Perbos J, Vincent P, Desai S, Haines B, Kuntsmann G (2003) The Jason-1 mission. Mar Geod 26(3–4):131–146

Sawyer DM, Vette JI (1976) AP-8 trapped proton environment for solar maximum and solar minimum, NSSDC/WDC-A-R&S 76–06, National Space Science Data Center, Report 76–06, Greenbelt

Tavernier G, Granier JP, Jayles C, Sengenes P, Rozo F (2003) The current evolutions of the DORIS system. Integr Space Geod Syst Satell Dyn Adv Space Res 31(8):1947–1952

Tavernier G, Fagard H, Feissel-Vernier M, Lemoine F, Noll C, Ries J, Soudarin L, Willis P (2005) The International DORIS Service (IDS). Adv Space Res 36(3):333–341. DOI 10.1016/j.asr.2005.03.102

Vette J (1991) The NASA/National Space Science Data Center trapped radiation environment model program (1964–1991). National Space Science Data Center, Report 91–29, Greenbelt

Vondrak J, Cepek A (2000) Combined smoothing method and its use in combining Earth orientation parameters measured by space techniques. Astron Astrophys 147(2):347–359

Willis P, Haines B, Bar-Sever Y, Bertiger W, Muellerschoen R, Kuang D, Desai S (2003) TOPEX/Jason combined GPS/DORIS orbit determination in the tandem phase. Adv Space Res 31(8):1941–1946. DOI 10.1016/S0273–1177(03)00156-X

Willis P, Haines B, Berthias JP, Sengenes P, Le Mouel JL (2004) Behaviour of the DORIS/Jason oscillator over the South Atlantic Anomaly. CR Geosci 336(9):839–846. DOI 10.1016/j.crte.2004.01.004

Willis P, Ries JC (2005) Defining a DORIS core network for Jason-1 precise orbit determination based on ITRF2000, methods and realization. J Geod 79(6–7):370–378. DOI 10.1007/s00190–005–0475–9